Tuning the functional properties of YBa2Cu3O7-δ by synchrotron x-ray irradiation

(Article begins on next page)

19 April 2024

Valentina Bonino, Lorenzo Mino, Angelo Agostino, Carmelo Prestipino, Matteo Fretto, and Marco Truccato

Tuning the functional properties of YBa2Cu3O7-δ by synchrotron X-ray irradiation

Tuning the functional properties of YBa$_2$Cu$_3$O$_{7-\delta}$ by synchrotron X-ray irradiation

Valentina Bonino[a], Lorenzo Mino[b], Angelo Agostino[b], Carmelo Prestipino[c], Matteo Fretto[d], Marco Truccato*

[a]Department of Physics, Interdepartmental Centre NIS, University of Torino, via Giuria 1, 10125 Torino, Italy; [b]Department of Chemistry, Interdepartmental Centre NIS, University of Torino, via Giuria 7, 10125 Torino, Italy; [c]University of Rennes 1, CNRS, ISCR (Institut des Sciences Chimiques de Rennes) -UMR 6226, F-35000 Rennes, France; [d]Nanofacility Piemonte INRiM (Istituto Nazionale di Ricerca Metrologica), Strada delle Cacce 91, 10135, Torino, Italy

*marco.truccato@unito.it; phone +390116707374

ABSTRACT

We investigated the electrical modifications induced by hard X-ray synchrotron radiation on the YBa$_2$Cu$_3$O$_{7-\delta}$ high temperature superconductor. We explored two different irradiation regimes. At low X-ray doses a progressive shift of the critical temperature of the superconductor has been obtained. Conversely, increasing the X-ray dose, a transition to a non-superconducting high resistance state is observed. These results pave the way to the realization of electrical devices by X-ray nanopatterning on this kind of oxide, extending the previous studies on Bi$_2$Sr$_2$CaCu$_2$O$_{8+\delta}$.

Keywords: synchrotron X-ray nano-beam, direct-write patterning, high-temperature superconductors, YBCO

1. INTRODUCTION

In the last years the quest for better photolithographic methods is pushing the use of increasingly smaller wavelengths for nanofabrication. For instance, with the 193 nm ArF excimer laser source a minimum feature size as small as 14 nm has been achieved.[1] Following this trend, X-ray sources have also been explored,[2] however the availability of suitable masks, problems in mask-wafer positioning, and diffraction effects, strongly limit the application of this technique.[3] In this respect, maskless methods based on hard X-ray sources could represent an interesting alternative. Although the need of X-ray sources having a high power density and a nanometric beam size requires the use of synchrotron facilities, the modification capability of hard X-rays has already been observed in different inorganic materials.[4, 5] For example, in low iron content soda lime silicate glasses, X-ray photo-induced reduction of iron has been detected.[6] Moreover, photo-induced phase transitions have also been observed in YBaFe$_4$O$_7$[7] and Pr$_{0.7}$Ca$_{0.3}$MnO$_3$.[8] Other interesting cases deal with the photo-induced nucleation.[9-11]

In this context, high temperature superconductor oxides play an important role since their functional properties can be tuned by irradiation with different kind of particles.[12-14] In particular, Bi$_2$Sr$_2$CaCu$_2$O$_{8+\delta}$ and YBa$_2$Cu$_3$O$_{7-\delta}$ high temperature superconductors, which are among the most studied high temperature superconductors, show a strong correlation between their electrical/structural properties and the non-stoichiometric oxygen content δ.[15-17] Moreover, the presence of intrinsic Josephson junctions,[18] originated from their peculiar crystallographic structure, has interesting applications in the THz technology.[19]

Concerning Bi$_2$Sr$_2$CaCu$_2$O$_{8+\delta}$, the non-stochiometric oxygen atoms, which are responsible for the superconducting properties of the material, are located in interstitial sites and are loosely bound[20-22] having a displacement threshold energy T$_d$=0.15 eV.[23] Thus, they can be easily removed by knock-on processes induced by X-ray irradiation. Indeed, our group already demonstrated that irradiating with high X-ray doses Bi$_2$Sr$_2$CaCu$_2$O$_{8+\delta}$ microcrystals it is possible to induce structural and electrical modifications, which can be correlated to a synergic effect of both crystal mosaicity increase and local oxygen depletion.[24-26]. Exploiting this effect, the material can be locally driven into a non-superconducting regime and it is possible to fabricate a Josephson device by means of direct-write X-ray nanopatterning.[27, 28]

In principle also YBa$_2$Cu$_3$O$_{7-\delta}$, which shows a Josephson plasma frequency higher than Bi$_2$Sr$_2$CaCu$_2$O$_{8+\delta}$, could be an interesting candidate for fabricating Josephson devices by modifying the local electrical properties of the material by X-

ray irradiation. However, the generation of oxygen vacancies in $YBa_2Cu_3O_{7-\delta}$ could be more difficult since the oxygen displacement energy is considerably higher than in $Bi_2Sr_2CaCu_2O_{8+\delta}$ (T_d= 3.45 eV).[29] Nevertheless, it has already been shown that an important fraction of oxygen can be displaced by means of 122 keV gamma irradiation through photo-induced oxygen knock-on.[30] In this contribution, starting from the encouraging results obtained by X-ray irradiation of $Bi_2Sr_2CaCu_2O_{8+\delta}$, we explore the possibility to extend the novel idea of direct-writing X-ray nanopatterning to $YBa_2Cu_3O_{7-\delta}$.

2. METHODOLOGY

2.1 Samples preparation and characterization

High quality $YBa_2Cu_3O_{7-\delta}$ microcrystals in the shape of whiskers have been synthesized with two synthesis methods based on different precursors. On one hand a combined used of Ca-, Al- and Te- precursor, as described in refs.[31, 32], has been adopted. This method promotes the growth of $YBa_2Cu_3O_{7-\delta}$ crystals having good superconducting properties (T_c = 79 - 84 K). On the other hand, Sb- precursor has been used improving the crystal purity and the critical temperature of the superconductor (T_c = 88 – 91 K), but at the expenses of a lower synthesis yield. With both synthesis methods, whisker-like crystals having shape of tapes are obtained with their length, width and height aligned along the a, b and c crystallographic directions. The crystal aspect ratio is 1000:10:1 along the a, b, and c axis, respectively. Whiskers with good crystal quality are selected for the fabrication of electrical devices allowing us to monitor the changes of $YBa_2Cu_3O_{7-\delta}$ functional properties after X-ray irradiation. Each selected crystal is mounted in a sapphire substrate with the c-axis perpendicular to the substrate. Four silver electrical contacts 2 µm thick are deposited via physical vapor deposition and annealed to 450 °C for 5 min in O_2 to ensure a low resistance of the contacts (see Figure 1). In this work two samples have been fabricated, one from each synthesis method. In the following sample A refers to the device based on a crystal synthesized with Ca-, Al- and Te- precursors, while sample B is the device obtained from the synthesis with Sb- precursor.
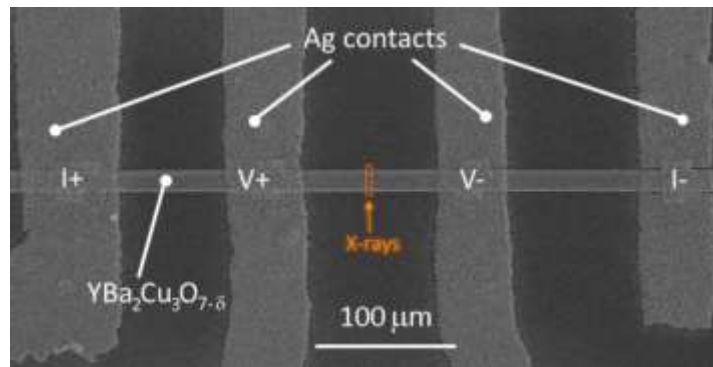

Figure 1 Scanning electron microscope (SEM) image of a typical $YBa_2Cu_3O_{7-\delta}$ electrical device with Ag contacts in four probe configuration. In order to monitor the electrical changes induced by the X-ray irradiation we exposed the region highlighted by the orange rectangle, which is located between the voltage contacts.

The final devices have been electrically characterized with a Janis ST-100 helium cryostat. The superconducting transition temperature ($T_{c,0}$), defined as the temperature at which a non-vanishing resistance value is observed beyond the noise level, has been determined from the R vs T curves.

2.2 Synchrotron X-ray setup and irradiation procedure

The $YBa_2Cu_3O_{7-\delta}$ micro-crystals were then irradiated at different X-ray doses between the voltage contacts (see Figure 1) and the corresponding R vs T curves where acquired after each irradiation step. Irradiations have been carried out in two different beamlines at the European Synchrotron Radiation Facility (ESRF). Sample A has been exposed in ID13 EHII hutch, placed at about 45 m from the source. The X-ray beam is focused by Be refractive lenses and a micrometric spot size of 2.0 × 2.5 µm² (horizontal × vertical) is achieved by means of Kirkpatrick-Baez mirrors.[33] The beam is

monochromatized at an energy $E_0 = 13.0$ keV with a double crystal monochromator. A photon flux $\Phi_0 = 4 \times 10^{11}$ ph s^{-1}, determined at the beginning of the experiment, corresponding to a power density $P_0 = 1.7 \times 10^8$ W m^{-2} is thus reached. Sample B was irradiated at the nanofocus beamline ID16B, placed at 165 m from the source, using a double white mirror and Kirkpatrick-Baez mirrors as nanofocusing optics to produce a beam with $E_0 = 17.4$ keV and $\Phi_0 = 2.9 \times 10^{11}$ ph s^{-1} [34]. At the experiment start, a spot size of 47×52 nm^2 (horizontal × vertical) was measured at the focal point. With these parameters a beam with $P_0 = 3.3 \times 10^{11}$ W m^{-2} is obtained. In both beamlines a sample stage combining a three-motorized translation axis with submicrometric resolution and an air-bearing stage for rotation are present.

The sample irradiation was performed aligning the beam parallel to the b-axis of the crystals and raster scanning the stage vertically and horizontally, along the [100] and the [001] crystallographic direction, in order to expose an entire section of the crystal. The exposed area was located between the voltage electrode and electrically characterized after the irradiation session. In sample A the effect induced by X-rays has been studied exposing for a prolonged time a crystal segment 5 μm long along the a-axis. Concerning sample B, using milder irradiation conditions, the modification induced to the superconducting behavior has been monitored after two irradiation steps, each one exposing a different segment of the crystal about 2 μm in length, 6.5 μm apart from each other. The step of the raster-scans was selected in order to have a small overlap between the beam profiles, such that a continuous and almost homogeneous profile of the irradiated regions should have been obtained. The X-ray exposure time for the two samples was tuned as a function of the beam conditions and of the observed modifications: exposure times of 1200 s/point and of 0.1 s/point were used for sample A and B, respectively.

For each irradiation step the absorbed dose has been calculated from the Beer-Lambert law as:

$$D = \frac{\Phi_0 \Delta t E_0 \eta}{m_\Phi} = \frac{\Phi_0 \Delta t E_0 \left(1 - e^{\frac{t}{\lambda_a}}\right)}{V_\Phi \rho} \tag{1}$$

where Δt is the irradiation time, and $m_\Phi = V_\Phi \rho$ are the mass, the volume and the density of the irradiated volume, respectively. The parameter η takes into account the exponential decaying profile of the absorbed X-rays inside the material, which is characterized by a geometrical depth t and an attenuation length λ_a. Given our experimental conditions, a λ_a of 21.08 μm and 35.25 μm are given for samples A and B respectively.

3. RESULTS AND DISCUSSION

Figure 2 shows the effect of an absorbed dose of 2.4×10^{12} Gy on sample A. After irradiation, we can notice a general increase in resistance and the electrical characteristic is dominated by a high resistance regime, although the superconducting behavior of the pristine state is still visible. From the orange curve in Figure 2a we can see that, below the superconducting transition at $T_{c,0} \sim 76$ K, a residual resistance of 14.5 Ω is still detected. The resistance progressively increases with lowering the temperature, highlighting a semiconducting behavior. Conversely, above the critical temperature the behavior is similar to the pristine state, showing a similar resistance increase passing from 76 to 220 K.

In order to appreciate the amount of the electrical modification induced in the irradiated portion of sample A, the resistivity change in this region has been estimated. Considering that the device resistance is the result of the two resistance in series, one coming from the pristine portion and the other arising from the irradiated region, the electrical resistivity of the irradiated material can be calculated starting from the R vs T curve in Figure 2a. Figure 2b shows the resistivity of the irradiated section estimated defining the X-ray interaction volume as the intersection between the exposed surface and the sample width (19.0 μm). An important increase of about 39 times in the resistivity with respect to the pristine state (~ 4 Ω μm) is observed at T = 220 K. This is an indication that the resistivity of the irradiated portion dominates the electrical resistance of the device. Indeed, the observed increase is bigger than the ratio between the length of the pristine and the irradiated regions (167 μm / 5 μm ≈ 33), implying that the contribution to the total electrical resistance originated from the irradiation portion of the crystal is greater than the one from the non-irradiated part. The huge increase in resistivity and the non-superconducting behavior of the portion of the sample region exposed to X-rays could be associated to a significant decrease of the oxygen content.[16, 35]
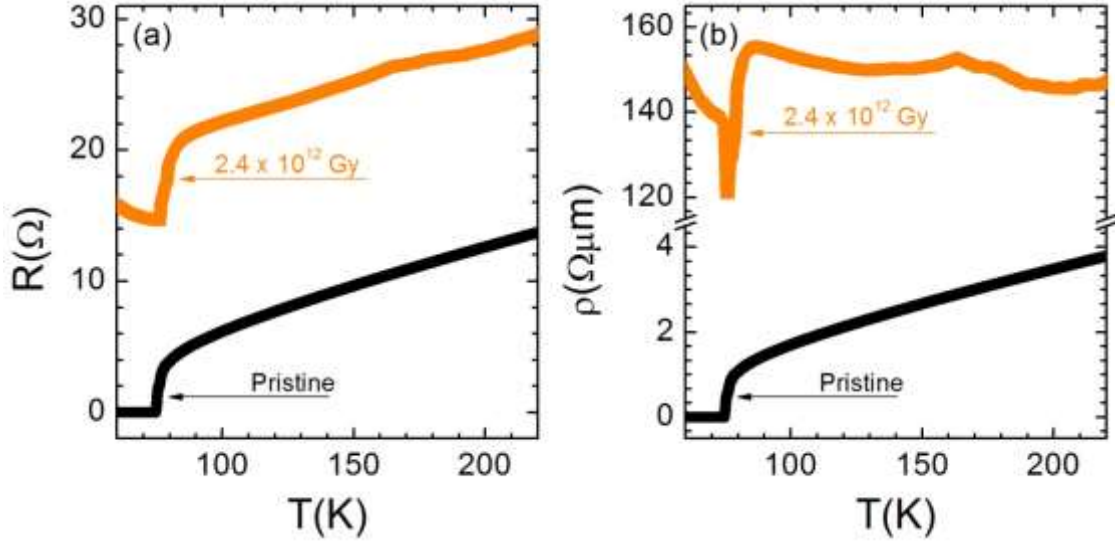
Figure 2. (a) Comparison of the electrical resistance versus temperature behavior, measured for sample A with the four-probe configuration, between the pristine state (black points) and after an X-ray absorbed dose of 2.4×10^{12} Gy (orange points). (b) The electrical resistivity of the irradiated $YBa_2Cu_3O_{7-\delta}$ region (orange points) of sample A is compared to the one of the pristine state (black points). Both behaviors have been calculated from panel (a).

According to our previous results obtained in $Bi_2Sr_2CaCu_2O_{8+\delta}$,[26, 27] using milder irradiation conditions, it should be possible to progressively modify the superconducting properties, locally tuning the oxygen content without reaching a semiconducting behavior. To confirm this hypothesis, we performed a new experiment on a similar sample (sample B) using the X-ray nanobeam available at the ESRF ID16B beamline to irradiate a smaller sample portion with lower doses (see Figure 3 for further details). Applying this irradiation strategy, we observed a modification of the device superconducting behavior for absorbed doses in the order of 10^{10}-10^{11} Gy. As it is reported in Figure 4a, although the shape of the resistance transition as a function of the temperature is almost preserved, an important shift of $T_{c,0}$ towards lower values takes place. The $T_{c,0}$ decreases from 91.2 K of the pristine state, to 89.7 K and 88.0 K after the irradiation of the first and the second portions respectively. The corresponding absorbed doses are reported for each step in Figure 4b. These variations in $T_{c,0}$, well beyond the experimental uncertainty, are remarkable considering that the shape of the superconducting transition has not changed. Indeed, in the R vs T curve the small irradiated portion was only expected to give rise to a non-vanishing resistance tail at the end of the main superconducting transition corresponding to the unaffected volume of the crystal.[26, 27] The strong influence induced in the superconducting general behavior suggests that the structural changes could extend beyond the 2 μm long irradiated area. However, from Figure 3 only a small local swelling, confined in the exposed area, is visible.
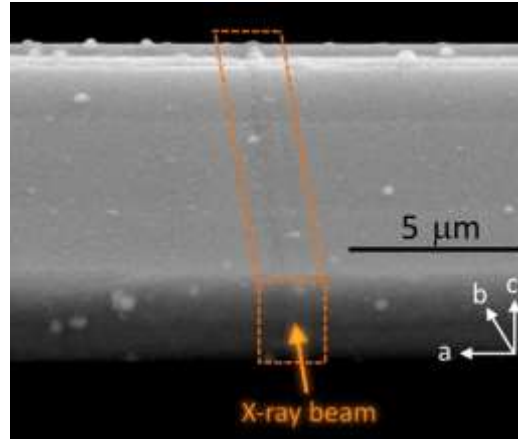
Figure 3. Scanning electron micrograph detail of the $YBa_2Cu_3O_{7-\delta}$ crystal region irradiated with X-rays (sample B). The nanobeam is aligned along the b-axis and scanned in the a-c plane to expose the volume highlighted in orange.

Combining the information obtained from sample A and B, $YBa_2Cu_3O_{7-\delta}$ microcrystals seems to be very sensitive to X-ray irradiation, to a major extent with respect to the $Bi_2Sr_2CaCu_2O_{8+\delta}$ compound previously studied. Given the strong correlation between the oxygen doping and the electrical properties of $YBa_2Cu_3O_{7-\delta}$, both the increase of the electrical resistivity and the decrease of the superconducting transition can be related to a reduction of the oxygen content. This phenomenon was explained in the past via a knock-on mechanism of the oxygen atoms. Indeed, it was shown by Piñera et al.[30] that a photon beam having an energy of 122 keV is able to displace a significant amount of O atoms in $YBa_2Cu_3O_{7-\delta}$ through this mechanism. Moreover, as it has been already demonstrated in $Bi_2Sr_2CaCu_2O_{8+\delta}$ whiskers [26], also an the increase of the crystal mosaicity could play a role. Indeed, the photoinduced formation of new grain boundaries could promote impurities segregation and variation of the oxygen content, a fact that could influence the behavior of the superconductor.[36] Finally, it cannot be excluded that internal stresses, possibly generated during the device fabrication step, are released via X-ray irradiation. This effect could also account for the extension of the structural modifications.
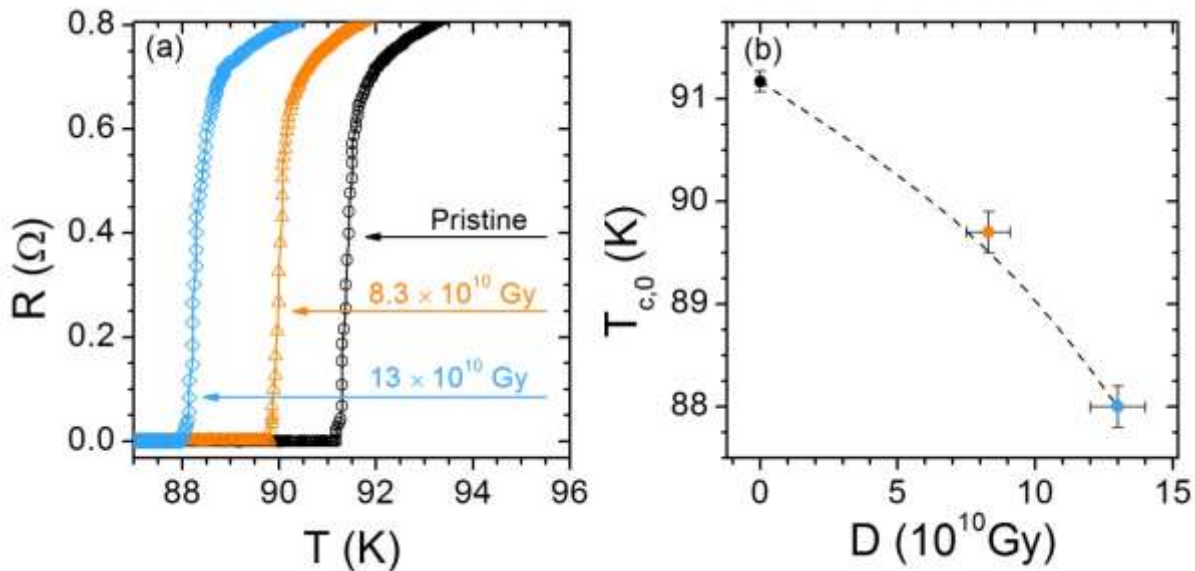

Figure 4. (a) Shift of the resistance transition measured, with a four-probe configuration, in sample B for pristine conditions (black circles) and after the first (orange triangles) and the second (light blue diamond) dose. (b) Critical temperature $T_{c,0}$ vs absorbed dose as determined from panel (a).

4. CONCLUSIONS

In the present study we have investigated the effects of hard X-ray irradiation in $YBa_2Cu_3O_{7-\delta}$ microcrystals by monitoring the electrical behavior as a function of the temperature. At low absorbed doses (10^{10}-10^{11} Gy), we were able to tailor the superconducting behavior inducing a progressive shift of the critical temperature from 91.2 K to 88.0 K. On the other hand, at higher absorbed doses (10^{12} Gy) the superconducting behavior of the irradiated portion is destroyed driving the material into a high resistance state, which shows a resistivity of about 150 Ω µm. These observations could be explained by an oxygen depletion phenomenon induced by photoelectron knock-on process. Moreover, the formation of grain boundaries during the irradiation could contribute to the observed changes. This study represents the first step to extend the X-ray nanopatterning process from $Bi_2Sr_2CaCu_2O_{8+\delta}$ to $YBa_2Cu_3O_{7-\delta}$. However, further structural investigations are needed to better understand the underlying mechanisms.

ACKNOWLEDGMENTS

REFERENCES

[1]   Seisyan, R. P., "Nanolithography in microelectronics: A review," Tech. Phys., 56(8), 1061-1073 (2011).

[2]   Ehrfeld, W., and Lehr, H., "Deep x-ray-lithography for the production of 3-dimensional microstructures from metals, polymers and ceramics," Radiat. Phys. Chem., 45(3), 349-365 (1995).

[3]   Maldonado, J. R., and Peckerar, M., "X-ray lithography: Some history, current status and future prospects," Microelectron. Eng., 161, 87-93 (2016).

[4]   Bras, W., and Stanley, H., "Unexpected effects in non crystalline materials exposed to X-ray radiation," J. Non-Cryst. Solids, 451, 153-160 (2016).

[5]   Mino, L., Borfecchia, E., Segura-Ruiz, J. et al., "Materials characterization by synchrotron x-ray microprobes and nanoprobes," Rev. Mod. Phys., 90(2), 65 (2018).

[6]   Ferreira, P. G., de Ligny, D., Lazzari, O. et al., "Photoreduction of iron by a synchrotron X-ray beam in low iron content soda-lime silicate glasses," Chem. Geol., 346, 106-112 (2013).

[7]   Duffort, V., Caignaert, V., Pralong, V. et al., "Photo-induced low temperature structural transition in the "114" $YBaFe_4O_7$ oxide," Solid State Commun., 182, 22-25 (2014).

[8]   Kiryukhin, V., Casa, D., Hill, J. P. et al., "An X-ray-induced insulator-metal transition in a magnetoresistive manganite," Nature, 386(6627), 813-815 (1997).

[9]   Tu, F., Spath, A., Drost, M. et al., "Exploring the fabrication of Co and Mn nanostructures with focused soft x-ray beam induced deposition," J. Vac. Sci. Technol. B, 35(3), (2017).

[10]   Hsu, P. C., Chen, Y. S., Hwu, Y. K. et al., "X-ray-induced Cu deposition and patterning on insulators at room temperature," J. Synchrot. Radiat., 22, 1524-1527 (2015).

[11]   Stanley, H. B., Banerjee, D., van Breemen, L. et al., "X-ray irradiation induced reduction and nanoclustering of lead in borosilicate glass," Crystengcomm, 16(39), 9331-9339 (2014).

[12]   Gupta, R. P., and Gupta, M., "Effect of radiation-induced oxygen disorder on the superconducting transition temperature in $YBa_2Cu_3O_7$ superconductors," Phys. Rev. Lett., 77(15), 3216-3219 (1996).

[13]   Tinchev, S. S., "Irradiation effects in YBCO thin films," J. Optoelectron. Adv. Mater., 7(3), 1253-1258 (2005).

[14]   Bandyopadhyay, S. K., Barat, P., Sen, P. et al., "Effect of alpha-irradiation on polycrystalline Bi-2223 superconductors," Physica C, 228(1-2), 109-114 (1994).

[15]   Watanabe, T., Fujii, T., and Matsuda, A., "Anisotropic resistivities of precisely oxygen controlled single-crystal $Bi_2Sr_2CaCu_2O_{8+\delta}$ systematic study on ``spin gap" effect," 79(11), 2113-2116 (1997).

[16]   Ito, T., Takenaka, K., and Uchida, S., "Systematic deviation from T-linear behavior in the inplane resistivity of $YBa_2Cu_3O_{7-y}$ - evidence for dominant spin scattering," Phys. Rev. Lett., 70(25), 3995-3998 (1993).

[17]   Cava, R. J., Hewat, A. W., Hewat, E. A. et al., "Structural anomalies, oxygen ordering and superconductivity in oxygen deficient $Ba_2YCu_3O_x$," Physica C, 165(5-6), 419-433 (1990).

[18]   Kleiner, R., and Muller, P., "Intrinsic josephson effects in high-T_c superconductors," Phys. Rev. B, 49(2), 1327-1341 (1994).

[19]   Ozyuzer, L., Koshelev, A. E., Kurter, C. et al., "Emission of coherent THz radiation from superconductors," Science, 318(5854), 1291-1293 (2007).

[20]   He, Y., Nunner, T. S., Hirschfeld, P. J. et al., "Local electronic structure of $Bi_2Sr_2CaCu_2O_8$ near oxygen dopants: A window on the high-T-c pairing mechanism," Phys. Rev. Lett., 96(19), (2006).

[21]   Runde, M., Routbort, J. L., Rothman, S. J. et al., "Tracer diffusion of oxygen in $Bi_2Sr_2CaCu_2O_x$," Phys. Rev. B, 45(13), 7375-7382 (1992).

[22]   Bandyopadhyay, S. K., Barat, P., Sen, P. et al., "Irradiation-induced oxygen knock-out and its role in bismuth cuprate superconductors," Phys. Rev. B, 58(22), 15135-15145 (1998).

[23]   Torsello, D., Mino, L., Bonino, V. et al., "Monte Carlo analysis of the oxygen knock-on effects induced by synchrotron x-ray radiation in the $Bi_2Sr_2CaCu_2O_{8+\delta}$ superconductor," Phys. Rev. Mater., 2(1), (2018).

[24]   Pagliero, A., Mino, L., Borfecchia, E. et al., "Doping Change in the Bi-2212 Superconductor Directly Induced by a Hard X-ray Nanobeam," Nano Lett., 14(3), 1583-1589 (2014).

[25]   Mino, L., Borfecchia, E., Agostino, A. et al., "Oxygen doping tuning in superconducting oxides by thermal annealing and hard X-ray irradiation," J. Electron Spectrosc. Relat. Phenom., 220, 69-75 (2017).

[26]   Bonino, V., Agostino, A., Prestipino, C. et al., "Structural and functional modifications induced by X-ray nanopatterning in Bi-2212 single crystals," 20(42), 6667-6676 (2018).

[27]   Truccato, M., Agostino, A., Borfecchia, E. et al., "Direct-Write X-ray Nanopatterning: A Proof of Concept Josephson Device on $Bi_2Sr_2CaCu_2O_{8+\delta}$ Superconducting Oxide," Nano Lett., 16(3), 1669-1674 (2016).

[28]   Mino, L., Bonino, V., Agostino, A. et al., "Maskless X-ray writing of electrical devices on a superconducting oxide with nanometer resolution and online process monitoring," Sci Rep, 7, 9066 (2017).

[29]   Bourdillon, A. J., and Tan, N. X., "Displacement damage in supported $YBa_2Cu_3O_{7-x}$ thin-films and finite-element simulations," Supercond. Sci. Technol., 8(7), 507-512 (1995).

[30]   Pinera, I., Cruz, C. M., Abreu, Y. et al., "Determination of atom displacement distribution in YBCO superconductors induced by gamma radiation," Phys. Status Solidi A-Appl. Mat., 204(7), 2279-2286 (2007).

[31]   Pascale, L., Truccato, M., Operti, L. et al., "Effect of Al and Ca co-doping, in the presence of Te, in superconducting YBCO whiskers growth," Acta Crystallogr. Sect. B-Struct. Sci.Cryst. Eng. Mat., 72, 702-708 (2016).

[32]   Calore, L., Khan, M. M. R., Cagliero, S. et al., "Al doping influence on crystal growth, structure and superconducting properties of $Y(Ca)Ba_2Cu_3O_{7-y}$ whiskers," J. Alloy. Compd., 551, 19-23 (2013).

[33]   Riekel, C., Burghammer, M., and Davies, R., "Progress in micro- and nano-diffraction at the ESRF ID13 beamline," 14, 012013 (2010).

[34]   Martinez-Criado, G., Villanova, J., Tucoulou, R. et al., "ID16B: a hard X-ray nanoprobe beamline at the ESRF for nano-analysis," J. Synchrot. Radiat., 23, 344-352 (2016).

[35]   Wuyts, B., Moshchalkov, V. V., and Bruynseraede, Y., "Resistivity and Hall effect of metallic oxygen-deficient $YBa_2Cu_3O_x$ films in the normal state," Phys. Rev. B, 53(14), 9418-9432 (1996).

[36]   Li, Q., Tsay, Y. N., Zhu, Y. et al., "Large T-c depression at low angle 100 tilt grain boundaries in bulk $Bi_2Sr_2CaCu_2O_{8+\delta}$ bicrystals," Appl. Phys. Lett., 70(9), 1164-1166 (1997).